Generalized fractional Fourier transform in optical systems

Yu.M.Kozlovskii

Institute for Condensed Matter Physics of the NAS of Ukraine,
1 Svientsitskii Str., 79011 Lviv, Ukraine E-mail: nesh@icmp.lviv.ua

Received: 29.07.2003

Abstract

We investigate the properties of intensity distribution of the two optical signals, which are shifted and modulated by a plane wave and correspond to the generalized fractional Fourier transform (FFT). The results of analytic and numerical calculations show the possibilities for designing new systems for the processing of information. As an example, the correlator based on the generalized FFT is considered. The domains of the generalized FFT in the practicable optical systems are obtained and analyzed. A principal possibility for the formation and recording of the interference pattern is demonstrated for the case when the images of the FFT, starting from the general form of the cascade matrix, are optically superimposed.

Key words: fractional Fourier transform, fractional correlation, cross shifting, image forming rectangular slit, ambiguity function

PACS: 42.30.K, 42.30.V, 42.79, 42.15.E, 42.25.F

1. Introduction

In last years, fractional Fourier transform (FFT) has been widely used in investigations of the existing systems for optical processing of information, as well as in the design of new such systems. By definition, FFT of an optical signal $f(x)$ is written in the form of integral transform [1-3]

$$u_p(x) = \hat{\Im}^p\left[f(x)\right] = \int f(x_1) K_p(x, x_1) dx_1, \qquad (1)$$

where

$$K_p(x) = C_\phi \exp\left(-i\frac{k[x^2 + y^2]}{2d_0 \tan\phi}\right) \times \exp\left(i\frac{kxy}{d_0 \sin\phi}\right), \qquad (2)$$

C_φ is the constant phase factor, $\hat{\Im}^p$ the FFT operator, $\varphi = p\pi/2$, and p the FFT-order parameter. At $p = 1$, a usual Fourier transform (FT) takes place. In the study [4], we have introduced the conjugate FFT $U_p(x) = \hat{\Im}^p\left[F\left(kx/d_0\right)\right]$. It is easy to see that the action of the operator $\hat{\Im}^p$ on the Fourier image of a signal yields in the conjugate fractional image.

The FFT methodology is closely related to the coordinate-frequency distribution (CFD) method. Usually, a Wigner distribution function is used in investigations of the FFT properties [5]. It has been shown that the rotation of the input signal on the middle conjugate coordinates corresponds to the FFT. The alternative method for the analytic description of optical signal properties in the FFT domain is based on the CFD of signals [6-7]. In particular, it is known that the input signal rotation on the informational diagram of the difference conjugate coordinates takes place proportionally to the FFT parameter p. The FFT image reconstruction is caused by action of the inverse

FT operator $\hat{\Im}^{-1}$ on the FFT distribution.

Both the methods stipulate a use of the rotation matrix $\mathbf{T}_\phi = [t_{ij}]$, corresponding to the linear transform of the conjugate coordinates $(x_0; \omega_0)$ of the input signal distribution. The coefficients of this matrix t_{ij} are limited values, since they are expressed through trigonometric functions $\sin\varphi$ and $\cos\varphi$. This fact essentially restricts the possibility for description of optical systems by the FFT methods. In particular, the distances between the elements of the optical system within such the approach can acquire a restricted series of values only, i.e. the superposition of two signals takes place in a restricted domain.

In the overwhelming majority of optical information processing systems, a case of two shifted optical signals is considered. The superposition in these systems occurs in the Fourier plane only. The FFT methodology makes it possible to investigate a signal superposition in the FFT domain or a fractional correlation. The first papers on the subject [5-6] have been devoted to the fractional correlation definition and the substantiation of its theoretical basis. The main deficiency of the existing joint transform correlator (JTC) lies in that the registration and investigation of the images concerns only to the Fourier plane. Another deficiency is associated with a difficulty of the interference pattern registration in the linear range. It leads to decreasing the signal/noise ratio and reducing the identification level.

In the study [7], the correlator based on the FFT has been proposed. The two concepts, those of the JTC and the FFT, have been combined together. Further development of the fractional correlator has been described in [8], where the case of two shifted signals (one of which is modulated by a plane wave ω_1) is considered. The principal scheme of the fractional correlator introduced in [9] is shown in Fig. 1.

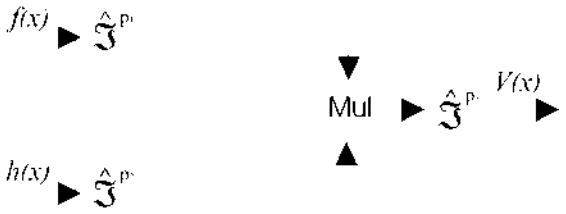

Fig. 1. Principal scheme of the fractional correlator.

The signals $f(x)$ and $h(x)$ are transformed in the system by the FFT of different orders p_1 and p_2. Then the signals are superimposed, with further creating the interference pattern. After performing the FFT of the p_3'th order and the usual FT, we can register the correlation function of the input signals. It is necessary to point out that, at $p_1 = p_2 = p_3$, we obtain the known JTC [10]. Note that the general condition linking the FFT orders at the input and output of the optical system is found in [7,8]:

$$\frac{1}{\tan\phi_1} - \frac{1}{\tan\phi_2} + \frac{1}{\tan\phi_3} = 0. \qquad (3)$$

The *ABCD*-matrix formalism, together with the FFT, has been considered in [11]. In frame of this formalism, the determinant of the matrix $\begin{pmatrix} A & B \\ C & D \end{pmatrix}$ is equal to unity, and three of four terms determine the image-forming conditions. An imperfection of such the approach is that this mechanism does not take into account the optical constants determining the distances between the elements of the optical system. The application of the approach to practicable optical systems should refer to a symmetric case only, when the distances in front of and behind of the lens are equal to each other.

It is important to increase the level of image protection and identification, while using the generalized FFT. Therefore, the subject of this paper is the investigation of general conditions of image forming. In particular, a use

of a general matrix A=[a_{ij}] with the elements equal to arbitrary values is proposed. Such the approach extends essentially the scope of the systems for optical processing of information that utilize the FFT methodology. The rotation matrix T_ϕ would then represent a particular case of the general matrix A.

As a result, a possibility appears for the construction of new devices for the optical information processing. In particular, this may be a correlator based on the FFT.

The plane of signal registration in the joint FFT domain at the fixed value of p_1 can be situated at arbitrary distance from the lens. The fact that this plane does not coincide with the focal plane essentially increases a dynamical range of intensities of the superimposed images. This allows one to register more exactly the spectrum of input signals on a sensitive material.

2. Images of the generalized FFT

For investigation of the FFT properties, the CFD may be used [3]. By definition, let us choose the base functionals in the form of ambiguity function $A_{ff}(x_0;\omega_0)$. As shown in [3], the FFT distribution $A_{ww*}(x_0;\omega_0)$ can be expressed in the following manner:

$$A_{ww*}(x_0;\omega_0) = \\ = A_{gg*}(a_{11}x_0 + a_{12}\omega_0; a_{21}x_0 + a_{22}\omega_0), \tag{4}$$

where the linear transform of the conjugate coordinates $(x_0;\omega_0)$ of the input signal distribution is described by the matrix A,

$$A = [a_{ij}] = \begin{pmatrix} a_{11} & -\frac{d_0}{k}a_{12} \\ \frac{k}{d_0}a_{21} & a_{22} \end{pmatrix}. \tag{5}$$

The determinant of this matrix is equal to unity. The advantage of the CFD method seen after inspecting formula (4) is that the operator $\hat{\Im}^{-1}$ reconstructs the FFT image:

$$|u_p(x)|^2 = \hat{\Im}^{-1}[A_{u_p u_p}(0;\omega_0)] = \\ \frac{1}{2\pi}\int A_{ff}\left(-\frac{d_0}{k}a_{12}\omega_0; a_{22}\omega_0\right)\exp(i\omega_0 x)d\omega_0. \tag{6}$$

It is easy to see that the two terms a_{12} and a_{22} determine the image-forming conditions. With formula (4), we obtain the relation for the light intensity distribution formed in the FFT plane:

$$|u_p(x)|^2 = \frac{1}{2\pi a_{12}}\times \\ \times\left|\int f(x_1)\exp\left(i\frac{ka_{22}}{2d_0a_{12}}x_1^2\right)\exp\left(-\frac{kxx_1}{d_0a_{12}}\right)dx_1\right|^2 \tag{7}$$

This intensity distribution can be detected experimentally. According to the definition (4), we have the generalized kernel of the FFT in the form of

$$K_\phi(x,y) = C_\phi\exp\left(-i\frac{k[x^2+y^2]}{2d_0}\frac{a_{22}}{a_{12}}\right)\times \\ \times\exp\left(i\frac{kxy}{d_0\alpha a_{12}}\right). \tag{8}$$

Comparing the FFT kernel (2) with the generalized one given by (8), we introduce the two coefficients that characterize the generalized kernel. First of them is the "effective" angle φ_{EF} of the rotation,

$$\tan\varphi_{EF} = \frac{a_{12}}{a_{22}}, \tag{9}$$

which is defined by the equation

$$m = a_{12}/\sin\varphi_{EF}. \tag{10}$$

It determines the rotation angle of the generalized FFT with respect to the FFT. The second coefficient is the scale factor that shows a scaling of the generalized FFT. Thus, we can conclude that the mentioned parameters relate the generalized and the usual FFTs.

The intensity distribution for the conjugate image [3] is as follows:

$$|U_p(x)|^2 = \frac{1}{2\pi a_{11}}\times \\ \times\left|\int f(x_1)\exp\left(i\frac{ka_{21}}{2d_0a_{11}}x_1^2\right)\exp\left(-\frac{kxx_1}{d_0a_{11}}\right)dx_1\right|^2 \tag{11}$$

Notice that the image-forming conditions in this case are determined by the two other components of the matrix $\boldsymbol{A}$ and the corresponding conjugate coefficients are

$$\tan\varphi^{CON}{}_{EF} = \frac{a_{11}}{a_{21}}, \qquad m^{CON} = \frac{a_{11}}{\sin\varphi^{CON}{}_{EF}} \ . \tag{12}$$

These coefficients relate the conjugate general and the conjugate FFTs.

3. Signal superposition in the generalized type of the FFT domain

General peculiarities of the signal superposition in the FFT domain were considered in [12] where the calculations were carried out for the case of the rotation matrix $\mathbf{T}_{\phi} = [t_{ij}]$. We combine here the two concepts of the signal superposition and the generalized FFT. By means of such the approach, we can find new regularities in the description of optical information processing systems.

Let us consider a general case of two (shifted and modulated by a plane wave) optical signals $f_1(x)$ and $f_2(x)$:

$$g(x) = f_1(x+b)\exp(i\omega_1 x) + f_2(x-b)\exp(-i\omega_1 x), \tag{13}$$

where b denotes the value of shift, $\omega_1 = \dfrac{2\pi\sin\theta}{\lambda}$ the spatial frequency, θ the angle of the incident plane wave. By virtue of linearity, the fractional Fourier image of the input signal (13) may be written as

$$|w_p(x)|^2 = |u_p(x;b,\omega_1)|^2 + |v_p(x;b,\omega_1)|^2 + i_p(x;b,\omega_1), \tag{14}$$

where $u_p(x;b,\omega_1)$ and $v_p(x;b,\omega_1)$ are fractional Fourier images of the shifted and the modulated signals. The calculations of the intensity distribution of the FFT diffraction pattern, based on formulae (9), (13) and (14), lead to

$$\begin{aligned} |w_p(x)|^2 = & \\ = \hat{\Im}^{-1}[A_{f_1 f_1^*}(a_{12}\omega_0; a_{22}\omega_0)\times & \\ \times\exp(i[a_{22}\omega_0 b + a_{12}\omega_0\omega_1])] + & \\ + \hat{\Im}^{-1}[A_{f_2 f_2^*}(a_{12}\omega_0; a_{22}\omega_0)\times & \\ \times\exp(-i[a_{22}\omega_0 b + a_{12}\omega_0\omega_1])] + & \\ + \hat{\Im}^{-1}[A_{f_1 f_2^*}(a_{12}\omega_0 + 2b;\ {}_{22}\omega_0 - 2\omega_1)] + & \\ + \hat{\Im}^{-1}[A_{f_1^* f_2}(a_{12}\omega_0 - 2b; a_{22}\omega_0 + 2\omega_1)]. & \end{aligned} \tag{15}$$

The two first terms in (15) form the FFT image of the two shifted signals:

$$|u_p(x;b,\omega_1)|^2 = \left|u_p\left(x + B_{FFT}\right)\right|^2, \tag{16}$$

$$|v_p(x;b,\omega_1)|^2 = \left|v_p\left(x - B_{FFT}\right)\right|^2. \tag{17}$$

Accordingly, the third and fourth terms in Eq.(15) form the interference term of the generalized FFT intensity distribution,

$$i_p(x;b,\omega_1) = u_p(x;b,\omega_1)v_p^*(x;b,\omega_1) + (u_p(x;b,\omega_1)v_p(x;b,\omega_1))^*, \tag{18}$$

where

$$u_p(x;b,\omega_1)v^*{}_p(x;b,\omega_1) = \exp\{2i\Omega_{FFT}x\}^* \quad u_p\left(x + B_{FFT}\right)v^*{}_p\left(x - B_{FFT}\right). \tag{19}$$

Making use of the results [15], we get the general formula describing the generalized FFT of the two shifted and modulated signals:

$$|w_p(x)|^2 = \left|u_p(x + B_\phi)\exp(i\Omega_\phi x) + v_p(x - B_\phi)\exp(-i\Omega_\phi x)\right|^2, \tag{20}$$

Relation (20) is equivalent to the form of the input signal (13). The generalized shifting parameter B_{FFT} and the modulation frequency Ω_{FFT} of the generalized FFT image are determined by the matrix equation:

$$\begin{pmatrix} B_{FFT} \\ \Omega_{FFT} \end{pmatrix} = \begin{pmatrix} a_{22} & -\dfrac{d_0}{k}a_{12} \\ -\dfrac{k}{d_0}\dfrac{1-a_{22}^2}{a_{12}} & a_{22} \end{pmatrix} \begin{pmatrix} b \\ \omega_1 \end{pmatrix}. \tag{21}$$

In this case the condition of superposition of the optical images takes the form

$$B_{FFT} = ba_{22} - \omega_1 \frac{d_0}{k} a_{12} = 0. \qquad (22)$$

The modulation frequency $\Omega_{FFT} = \omega_1 a_{22} - b\frac{k}{d_0}\frac{(1-a_{22}^2)}{a_{12}}$ appears to be maximal under this condition. The input images superimpose at the point that corresponds to the angle φ_{EF}.

4. General peculiarities of generalized FFT realization in optical systems

The registration of the two optically superimposed images in the FFT domain is achieved due to illumination with the two mutually coherent beams having their plane wave fronts aligned at the fixed angle one to the other.

The functional scheme of the optical correlator consists of the two parts: the system for the interference pattern registration (Fig.2,(1)) and the FFT block (Fig.2,(2)).

The system for the interference pattern registration (Fig.2, (1)) consists of the following elements: the illumination system; the input image, *Image 1*; the reference image, *Image 2*; and the optical system of the FFT.

The illumination system forms the two reference waves and consists of the first pair of two identical lenses, *Lens 1* and *Lens 2,* with their focal distances equal to F_1, and the second pair of the identical lenses, *Lens 3* and *Lens 4,* with the focal distances F_2. The distance between the two pairs of lenses is equal to F_1+F_2. The intervals between the pairs of lenses (*Lens 1, Lens 2* and *Lens 3*, *Lens 4*) are covered by the opaque screens. Since the lenses *Lens 1* and *Lens 2* are displaced by the distance L_1, and the lenses *Lens 3* and *Lens 4* by the distance L_2, then the shift of the optical axes of *Lens 1*, *Lens 3* and *Lens 2*, *Lens 4* by the distance $\Delta=(L_1-L_2)/2$ is achieved along the direction of propagation of the plane waves.

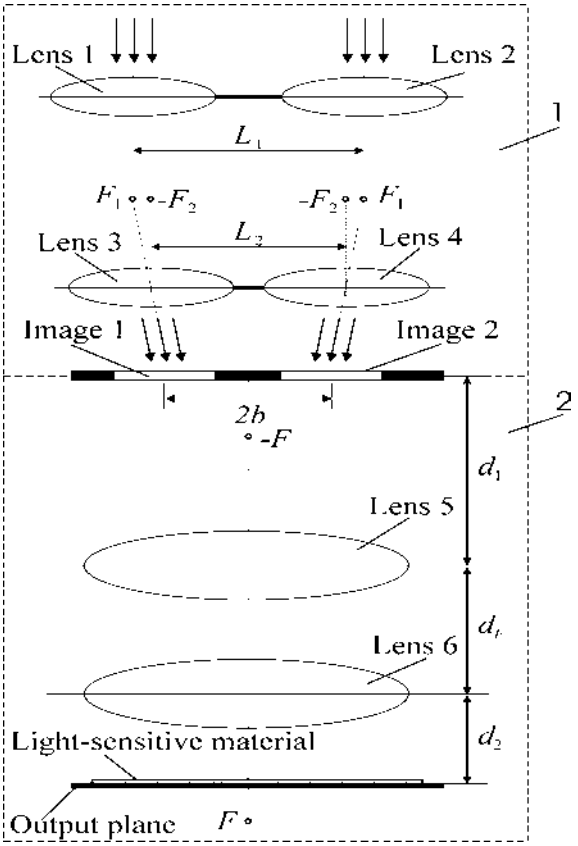

Fig. 2. Scheme of the JFC.

Due to this shift of the optical axes of the pair lenses, the two reference plane waves are formed at the output of the illumination system. The waves propagate symmetrically to the axis of the optical correlator at the angle defined by $\sin\theta = \Delta/F_2$. Thus, the two symmetrical reference plane waves $A_1(x) = A_0 \exp(ik \sin\theta x)$ and $A_2(x) = A_0 \exp(-ik \sin\theta x)$ are formed in the illumination system, with the fixed angle θ, where A_0 is a constant phase factor.

This illumination system has a peculiarity such that the sign of the angle θ may be changed. Under the condition $L_1>L_2$, the two converging reference plane waves are formed at the output. The waves are characterized by the angle $\theta > 0$. When $L_1<L_2$, the divergent reference plane waves are formed, characterized by the angle $\theta < 0$. When the reference plane waves propagate in the same plane, the input image, i.e. *Image 2,* is displaced. The image is described by the function of amplitude

transmission $f_1(x,y)$ and is illuminated by the reference plane wave $A_1(x)$. The reference image, *Image 1*, described by the amplitude transmission function $f_2(x,y)$, is illuminated by the other reference plane wave $A_2(x)$. As a result, the optical signal is formed at the output of the optical correlator system (see (13)):

$$f(x,y) = f_1(x+b,y)\exp\left(i\Omega_{ref}x\right) + f_2(x-b,y)\exp\left(-i\Omega_{ref}x\right), \quad (23)$$

where b is the value of the relative cross shifting of the *Images 1, 2*, and $\Omega_{ref} = k\sin\theta$ the spatial frequency of the reference wave determined by the angle θ. The FFT optical system of the input signal (23) consists of *Lens 5*, or *Lens 5* and *Lens 6* with the focal distance F disposed at the distance $d_F = D_F/F$ along the optical axis. The plane of *Lens 5* is displaced by $d_1 = D_1/F$ from the plane of the input and reference images (*Images 1* and *2*). The interference pattern of the FFT signal (23) is formed at the distance $d_2 = D_2/F$ behind the *Lens 6* in the output plane.

The important novelty of such the correlator consists in the fact that the generalized FFT is optically realized with the aid of one or two optical stages and at the arbitrary distances d_1 and d_2 in the output plane.

The main difference of this scheme from the others is that the formation of the high-visibility pattern with the spatial frequency Ω_{FFT} takes place in the generalized FFT domain, where the spatial frequency of the interference pattern is defined by

$$\Omega_{FFT} = \frac{\Omega_{ref}}{a_{22}}. \quad (24)$$

If the "effective" angle of rotation φ_{EF} is used, then the theoretical restriction $|a_{ij}| \le 1$ of such the transformation imposed on the geometrical parameter of the stage is removed.

The advantage of the suggested scheme of correlator based on the generalized FFT consists in the possibility of realization of "effective" rotation angle φ_{EF} values at different distances d_1 and d_2. This means that one can form the interference pattern with the given spatial frequency Ω_{FFT} at the recording stage.

Taking into account that the matrix coefficients a_{12} and a_{22} are determined by different relations and each of these coefficients can be both positive and negative, we are able to realize four different domains of the generalized FFT input images.

5. Domains of generalized FFT realization in the optical stage with one lens

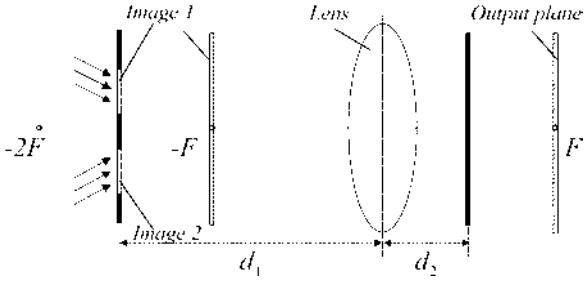

Fig. 3. Scheme of the generalized FFT realization in optical stage.

In order to investigate the approach in a more detail, let us consider different domains of the generalized FFT. For this purpose we elucidate the physical meaning of the invariant parameters a_{ij}. Fig.3 illustrates a general scheme for realization of the generalized FFT in the optical stage. The matrix of this stage is [13-14]

$$M_{CAS} = \begin{pmatrix} 1-d_1 & -\frac{d_0}{k}(d_1+d_2-d_1d_2) \\ \frac{k}{d_0} & 1-d_2 \end{pmatrix}. \quad (25)$$

The invariant parameters are given by the relations

$$a_{12} = d_1(1-d_1)+d_2,\ a_{22} = 1-d_2 \quad (26)$$

The matrix (25) for the FFT takes the following form:

$$M_{CAS} = \begin{pmatrix} \cos\varphi & -\frac{d_0}{k}\sin^2\varphi \\ \frac{k}{d_0} & \cos\varphi \end{pmatrix}. \qquad (27)$$

This matrix allows one to realize only a symmetric case ($d_1 = d_2 = d$), with the distances restricted by *2F*. Due to the form of the generalized matrix (5), a non-symmetric case ($d_1 \neq d_2$) can be considered for the generalized FFT. Superposition of the input signals is realized for the arbitrary distances both before and behind the lens.

Let us describe a methodology for the stage parameter calculations at the optical superposition of the input images. For the given optical stage, the elements a_{12} and a_{22} of matrix (5) (i.e., the invariant parameters of such the stage) should be calculated, where the "effective" rotation angle φ_{EF} at the generalized FFT is defined from (9). The expediency of using the "effective" rotation angle is caused by the fact that the rotation matrix $\mathbf{T}_{\varphi} = \| t_{ij} \|$ cannot be realized in optical stage. Knowing the angle φ_{EF}, one can calculate the value of the relative distance d_1 from the input plane and the corresponding value of the relative distance d_2 to the output plane of the optical stage.

The signs of the invariant coefficients determine the domain of the FFT realization. Let us consider a "motion" of the images on the informational diagram. Each domain (see Fig.4) has the two boundary points. The FFT domain is placed between these points. One can see that any point on the informational diagram would have a certain corresponding construction of the optical stage, where the generalized FFT is realized. The first domain of the generalized FFT image formation corresponds to the values of the FFT parameter in the range of $0 < p < 1$ (Fig. 4a). The extreme cases of $p = 0$ (the coordinate plane) and $p = 1$ (the frequency plane) correspond to the usual FT.

The FFT domain is placed between these planes and the FFT parameter in this domain changes continuously from 0 to 1. Such the domain is described by the matrix (5), under the conditions when the invariant parameters are $a_{12} > 0$ and $a_{22} > 0$. The distance d_2 changes from a zero up to the focal distance of the lens *F*, whereas d_1 may be arbitrary. The boundary points of this domain are $p = 1$ and $p = 2$. The point $p = 1$ is peculiar, i.e. it corresponds to the usual FT ($a_{22} = 0$). At the fixed position of the output plane, the input plane can be placed differently, with the corresponding distances determined by the condition $a_{12} > 0$.

At the point $p = 2$, the inverse image of the input signal is formed, whereas the conjugate FFT is formed in the domain between the extreme points $p = 1$ and $p = 2$. Then the distance d_2 would change from *F* to the infinity and $d_1 > d_2/(d_1 - 1)$. It is important to note that using of matrix (5) leads to scaling the inverse image at the point $p = 2$, the effect being determined by the matrix $\begin{pmatrix} -m & 0 \\ 0 & -1/m \end{pmatrix}$. This matrix is unitary if the T_{ϕ} matrix is used. The peculiarities on the informational diagram are caused by the lack of the transform to the points $p = 3$ and $p = 4(0)$, since $d_2 < 0$ in this case. On the other hand, there exists a third domain of the generalized FFT, describing the inverse image of the input signal. In this case d_2 is larger than *F* and $d_1 < d_2/(d_1 - 1)$.

Let us consider the optical system with the parameters $a = 1,\ b = 2,\ d = 250$.

Domain 1:

$d_1 = 2.5, \quad d_2 = 0.5, \quad a_{12} = 1.75, \quad a_{22} = 0.5.$

The parameter p changes continuously from 0 to 1 for the region between the points $p = 0$ and $p = 1$ and it is therefore possible to record a high-contrast interference pattern at different values of the "effective" rotation angle φ_{EF}. Owing to use of the generalized FFT methodology, we may also record the images on the different scales at the arbitrary values of the spatial frequency. So, a large number of modifications may exist for the realization of optical correlator in this system.

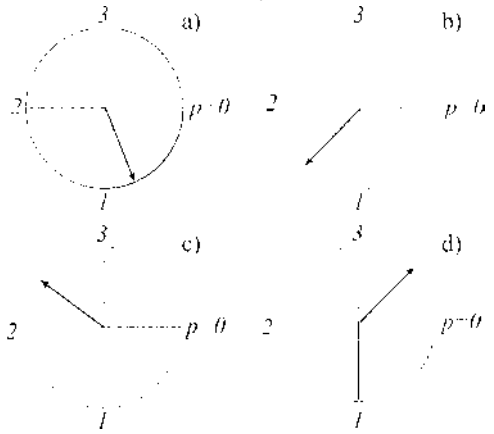

Fig. 4. Domains of the generalized FFT realization.

Fig. 5(I) illustrates the light intensity distribution for the generalized FFT realization at the superposition point corresponding to Domain 1 (Fig. 4a). The images in this case are superimposed at the value of the "effective" rotation angle $\phi = 74^0$. In such the system, the following intensity distribution is formed in the output plane of the generalized FFT images:

$$\left|u_p(x,y)\right|^2 = 4\left|u_p^{(1)}(x,y)\right|^2 \cos^2\left(\Omega_{FFT}\, x\right). \qquad (28)$$

This relation reveals the two superimposed fractional images of the slits, which are modulated by the high-contrast periodic interference pattern with the 100% contrast ratio.

Domain 2:

$d_1 = 1.5, \quad d_2 = 1, \quad a_{12} = 1, \quad a_{22} = -0.5.$

If we change the distances between the optical elements in the system (Fig. 3), the parameter a_{22} changes its sign and the superposition of the input signals takes place in the Domain 2 ($1 < p < 2$; $a_{12} > 0$ and $a_{22} < 0$, see Fig. 4b) of the generalized FFT realization. This system corresponds to the conjugate generalized FFT and the corresponding intensity distribution is shown in Fig. 5(II).

The main feature of this stage scheme is that the optical superposition of the generalized FFT images occurs under illumination of the input images (*Image 1* and *Image 2*) by the divergent ($\theta < 0$) reference waves. The other feature of the latter scheme is that the corresponding input plane exists at the condition a_{12}=0 for the output plane. Then the output plane may be used as an image plane and the inverse image with the scale factor $m > 1$ may be formed in this plane. The boundary value of the parameter $p = 2$ corresponds to the mutual position of the coordinate planes on the informational diagram.

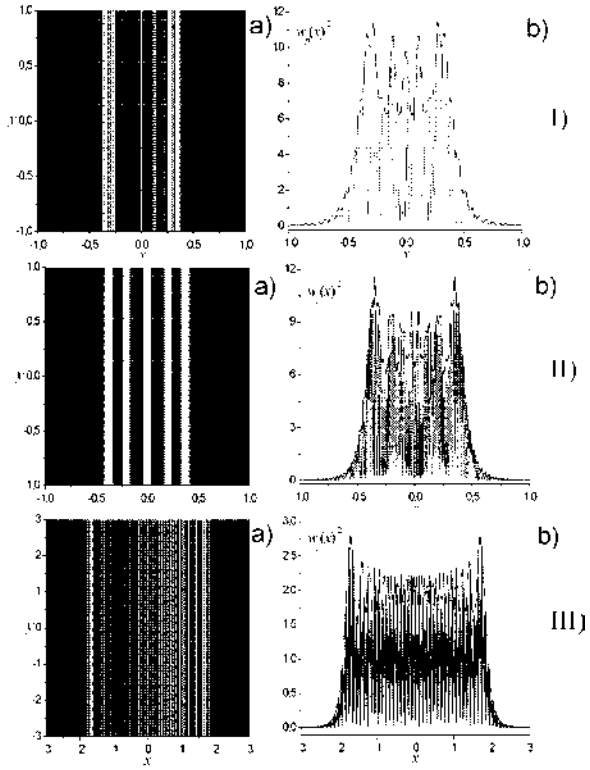

Fig. 5. Intensity distribution of the generalized FFT images at the superposition point in optical stage.

The interference pattern of the optically superimposed generalized FFT images is also registered in the output plane:

$$\left|U_p(x,y)\right|^2 = 4\left|U_p^{(1)}(x,y)\right|^2 \cos^2(\Omega_{FFT}x). \quad (29)$$

When compare with Domain 1, the superimposed images of the generalized FFT are less contrast and scaled-up ($m > 1$).

Domain 3:

$d_1 = 2, \quad d_1 = 3, \quad a_{12} = -1, \quad a_{22} = -2.$

With the above values of the parameters of optical system, the inverse image of the generalized FFT is formed, which corresponds to Domain 3 (see Fig. 4c), where the values of the parameters are $2 < p < 3$ ($a_{12} < 0$ and $a_{22} < 0$). Formation of the inverse image with the value of the scale factor $m = 1$ corresponds to the case of $p = 2$.

The optical superposition of the inverse images of generalized FFT takes place at the value of $\sin\theta = 0.06$ for the convergent reference waves and the "effective" rotation angle $\varphi_{EF} = 27^0$.

The corresponding intensity distribution of the inverse image of generalized FFT is shown in Fig. 5(III).

Domain 4: $a_{12} < 0; \quad a_{22} > 0.$.

This domain (see Fig. 4d) cannot be realized in optical stage, because the distance d_1 becomes negative ($d_1 < 0$) and lacks a physical meaning.

6. Domains of generalized FFT realization in the double optical stage

Let us analyze the system based on a double-stage optical system. The general scheme of the generalized FFT realization for this case is shown in Fig.6.

We point out that the additional parameter d_F appears for this system, improving a safety of devices for the information protection. Let us write the expression for the double-stage matrix:

$$M_{D\_CAS} = M_{CAS} \times ML_2 \times M_{SP}, \quad (30)$$

where $M_{L2} = \begin{pmatrix} 1 & 0 \\ F/k & 1 \end{pmatrix}$, $M_{SP} = \begin{pmatrix} 1 & -F \setminus k \\ 0 & 1 \end{pmatrix}$

and F is the focal distance. The invariant parameters may be calculated with the relations

$$\begin{aligned} a_{12} &= d_2(1-d_1)+(1-d_2)[d_1(1-d_F)+d_F]; \\ a_{22} &= (1-d_2)(1-d_F)-d_2. \end{aligned} \quad (31)$$

A characteristic feature of the double stage is that only this system allows realizing the FFT by the definition. Let us consider the generalized FFT realization scheme in the double-stage system, when the parameters are $a = 1$, $b = 3$ and $F = 100$.

Domain 1:

$d_1 = 4.5, \quad d_2 = 2.5, \quad d_F = 3,$

$a_{12} = 0.25, \quad a_{22} = 0.5.$

This scheme corresponds to F=0+F+0, where F is the focal distance.

The superposition points changing from zero up to F correspond to the generalized FFT domain. The numerical results for the two-slit superposition and the rotation angle $\phi = 27^0$ are shown in Fig. 7(I). They describe Domain 1, where the FFT image is formed.

Domain 2:

$d_1 = 0.2, \quad d_2 = 1.35, \quad d_F = 3.5,$

$a_{12} = 0.03, \quad a_{22} = -0.47.$

For this scheme we consider the stage construction 4F=F+2F+F, when the generalized FFT changes in the domain 4F=0..F+2F+0..F. In this case the superposition occurs at the value of the "effective" rotation angle $\phi = 4^0$ (see Fig. 7(II)). In Domain 2 (see Fig.4b), the generalized conjugate image is formed.

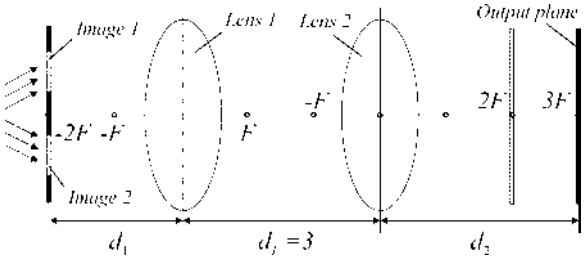

Fig 6. The FFT realization scheme in the double optical stage.

Domain 3:

$d_1 = 5.3, \quad d_2 = 1.25, \quad d_F = 4,$

$a_{12} = -2.4, \quad a_{22} = 0.5.$

Here the FFT domain is 4F or 4F=F..2F+F..2F. The intensity distribution of the superimposed slits for the "effective" rotation angle $\phi = 78^0$ (see Fig. 7(III)) takes place in the domain $2 < p < 3$ (see Fig.4c). In this domain the inverse image is formed.

Domain 4:

$d_1 = 1.75, \quad d_2 = 2.5, \quad d_F = 3$

$a_{12} = -1.25, \quad a_{22} = 0.5.$

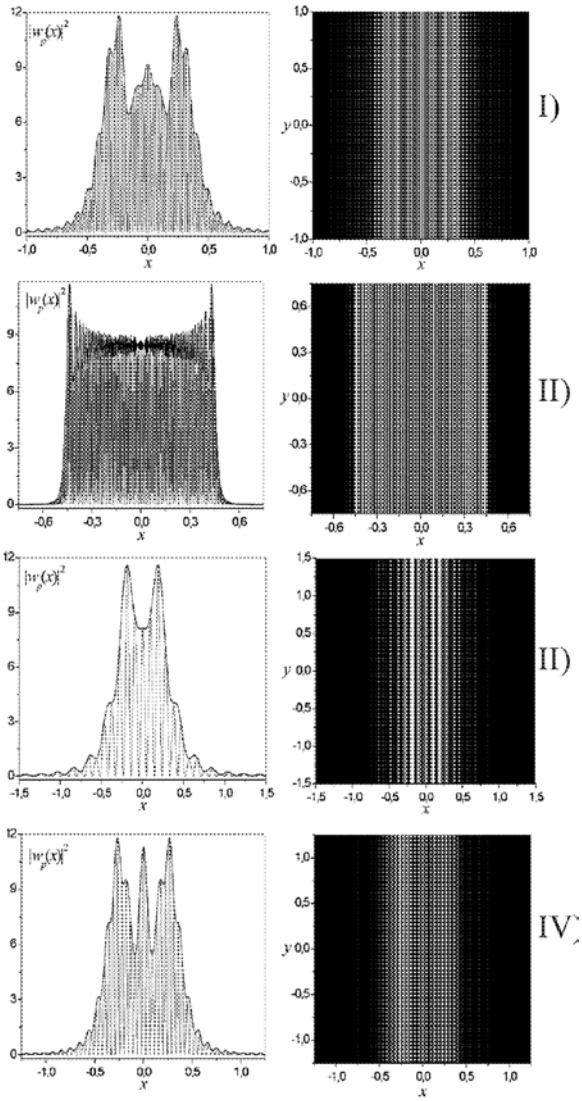

Fig. 7. Intensity distribution of the generalized FFT images at the superposition point in the double optical stage.

With the above parameters, the scheme is 7F=2F+3F+2F and the fractional domain is 2F..+3F+2F. Here the superposition occurs for the "effective" rotation angle $\phi = 65^0$ (see Fig. 7(IV)) and in the domain of $3 < p < 4(0)$ (see Fig. 4d), where the generalized conjugate inverse FFT image is formed.

7. Conclusions

The main purpose of this paper has been to show the advantages and principal possibilities of the systems for optical information processing, which appear owing to use of the generalized matrix A_{ij}. Based on this matrix, the generalized FFT is constructed. The main advantage of this approach consists in the possibility for the matrix coefficients to acquire arbitrary values. The parameters of the optical systems are calculated, using the invariant parameters a_{ij}, which are the elements of the matrix A_{ij}. Utilization of the generalized FFT has allowed us to improve the existing information processing systems and construct new systems of this type. In particular, the example for the correlator based on the generalized FFT clearly shows this possibility.

7. References

1. Namias V. J. Instr. Maths Applics., **25** (1980) 241-265.
2. Ozaktas H.M., Mendlovic D. Opt. Commun., **101** (1993) 163-169.
3. Shovgenyuk M. V., Kozlovskii Yu.M. Preprint ICMP-01-05U, Lviv, (2001) 42 p (in Ukrainian).
4. Shovgenyuk M. V., Kozlovskii Yu.M. Dep. NAS Ukraine, **6** (2000) 92-97 (in Ukrainian).
5. Lohmann A.W. J. Opt. Soc. Am. **10** (1993) 2181-2186
6. Mendlovic D., Ozaktas H., Lohmann A., J. Opt. Soc. Am. 34 (1995) 303-309
7. Granieri S., Arizaga R., Sicre E., Appl. Opt., **36** (1997) 6636-6645.
8. Lohmann A.W., Mendlovic D., Appl. Opt.,

36 (1997) 7402-7407.
9. Kuo C. J., Luo Y. Appl. Opt., **37** (1998) 8270-8276.
10. Jin S., Lee S. Opt. Commun., **207** (2002) 161-168.
11. Weaver C., Goodman J. Appl. Opt., **5** (1966) 1234-1249.
12. Shovgenyuk M. V., Kozlovskii Yu.M., Muravsky L., Fitio V. Ukr. J. Phys. Opt. **3** (2002) 106-115
13. Shovgenyuk M. V., Kozlovskii Yu.M. Phys. Collection of Shevchenko Sci. Soc. (Lviv), **4** (2001) 289-306 (in Ukrainian).
14. Shovgenyuk M. V., Kozlovskii Yu.M. Proc. 2nd Int. Smakula's Symp., Ternopil, (2000) 86 (in Ukrainian).